Lecture 2

Phase Turbulence in Convection

F. H. Busse

Notes by by L. Lu and F. Pétrélis

1 Description of the Rayleigh Bénard instability

1.1 Mechanism

When a fluid layer is heated from below, a fluid particle at the bottom of the layer is hotter than the one above her. Consequently it is lighter and has a tendency to go up which is slowed down by the viscous force. This is the mechanism of the Rayleigh Bénard instability which can generate convection movements in a fluid heated from below. By comparing the power of the two forces involved in this mechanism, we can get an idea of a parameter which controls the instability development.

We first have to specify how the density ρ of the fluid depends on its temperature. The simplest hypothesis is to use a first order approximation and to assume a linear dependency that yields

$$\rho = \rho_0 \left(1 - \gamma(T - T_0)\right), \tag{1}$$

where ρ_0 is the density at temperature T_0 and γ is the expansion coefficient

$$\gamma = \frac{1}{V}\frac{\partial V}{\partial T}_P = -\frac{1}{\rho}\frac{\partial \rho}{\partial T}_p . \tag{2}$$

This is part of the Boussinesq approximation, pertinent for almost all common cases of Rayleigh Bénard instability.

We can estimate the buoyancy force F_b per unit volume between the bottom of the layer at temperature T_2 and the top at temperature T_1 (with $T_1 < T_2$). Using the height d between the two surfaces of the layer (see fig 1), we get $F_b = \rho_0\,\gamma\,(T_2 - T_1)\,g\frac{V\,d}{\kappa}$. The last coefficient $\frac{V\,d}{\kappa}$ where V is the velocity of the fluid and κ the thermal diffusivity takes into account the effect of the thermal diffusion on the distortion of constant density planes. We compute the power of this buoyancy force per unit volume L_p by multiplying it with the velocity and we obtain

$$L_p = c_1\,\rho_0\,\gamma\,(T_2 - T_1)\,g\,d\,\frac{V^2}{\kappa}, \tag{3}$$

where c_1 is a numerical coefficient.

The power of the viscous force per unit volume is the product of the force per unit volume $\rho_0\,\nu\,\nabla^2\,V \simeq \rho_0\,\nu\,\frac{V}{d^2}$ with the velocity

$$L_d = c_2\,\rho_0\,\nu\,\frac{V}{d^2}V, \tag{4}$$

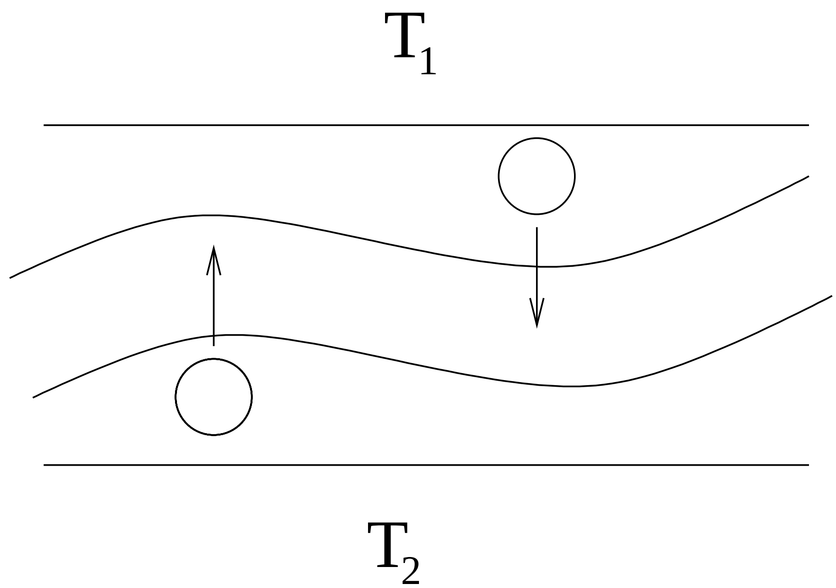

Figure 1: Sketch of layer heated from below at temperature T_2 greater than the top surface temperature T_1.

c_2 is also a numerical coefficient. When the ratio between these two powers exceeds a critical value convection occurs. We define the Rayleigh number by

$$R = \frac{L_p\, c_2}{L_d\, c_1} = \frac{\gamma\,(T_2 - T_1)\, g\, d^3}{\nu\, \kappa}\,, \tag{5}$$

and its value at onset is the critical Rayleigh number $R_c = \frac{c_2}{c_1}$.

1.2 Interesting aspects

The study of convection phenomena concerns a very wide range of systems. Varying the Prandtl number (ratio between the kinetic viscosity and the thermal diffusivity) and other parameters (related to other effects such as magnetic field or rotation...) lots of situations can arise. Some of them are presented in figure 2.

A particularity of the usual convective instability is that the unstable mode is degenerate at onset. We will show in the following paragraph that the horizontal isotropy of the forcing exists and that the manifold of the unstable modes is characterized by wave vectors of fixed norm but free direction in the xy plane. As we can see in figure 3, this is really different from an instability generating a unique unstable mode and leads to some new behaviour on which we will now focus on.

1.3 Onset of Instability

The full set of equations describing the motion of a fluid is as follows:

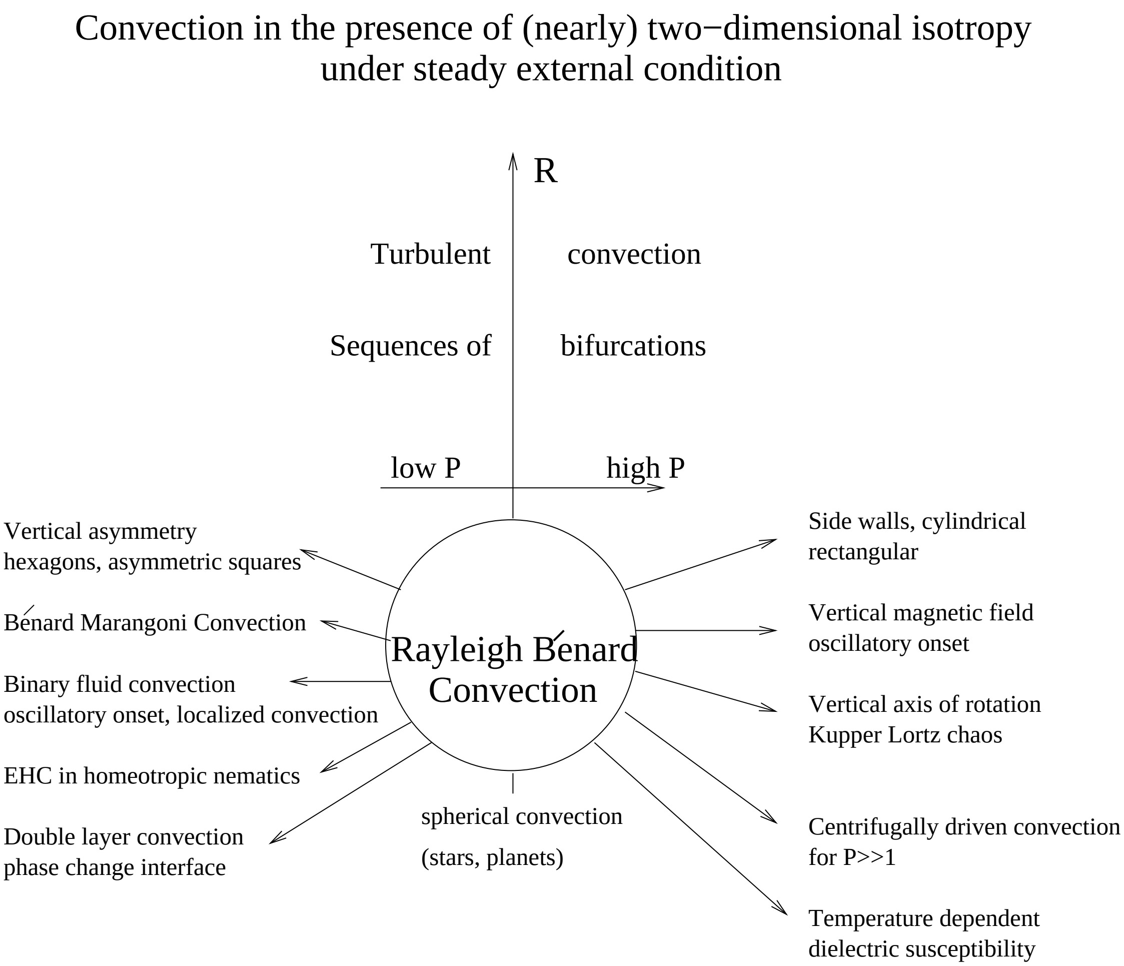

Figure 2: Some effects that occur in Rayleigh-Bénard convection.

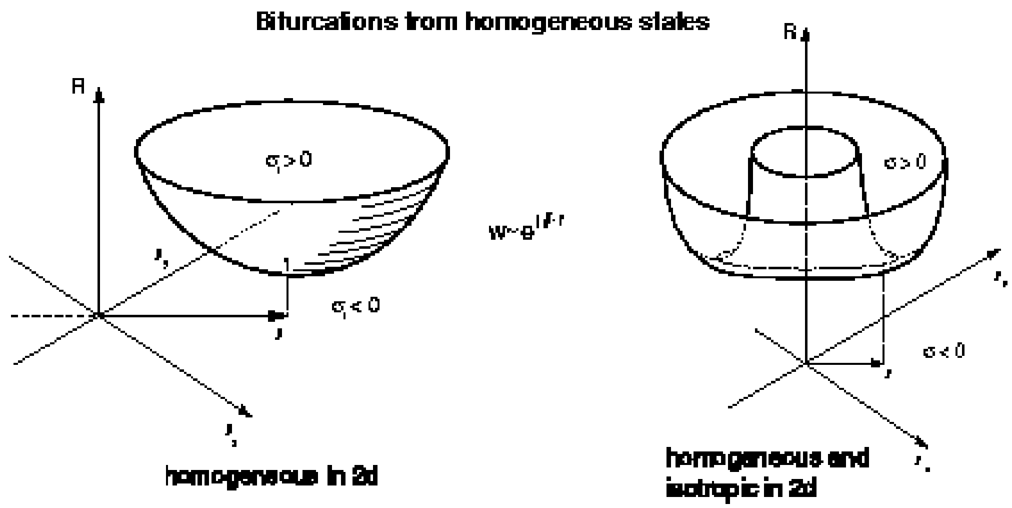

Figure 3: Critical Rayleigh number R at onset of instability for a horizontal wave vector (k_x, k_y) in a non-isotropic case and in an isotropic one.

$$\frac{\partial}{\partial t}\rho + \partial_j \rho u_j = 0 \tag{6a}$$

$$\rho \frac{d}{dt} u_i = \rho \frac{\partial}{\partial t} u_i + \rho u_j \partial_j u_i = -\partial_i p - \rho g k_i + \partial_j [\nu \rho (\partial_i u_j + \partial_j u_i - \frac{2}{3} \delta_{ij} \partial_k u_k)] \tag{6b}$$

$$\rho T \frac{ds}{dt} = \rho c_p \frac{dT}{dt} + \frac{T}{\rho} \left(\frac{\partial \rho}{\partial T} \right)_p \frac{dp}{dt} = \partial_j (\lambda \partial_j T) + \Phi \tag{6c}$$

where Φ is mechanical dissipation and the density ρ has a temperature dependence given by

$$\rho = \rho_0 (1 - \gamma (T - T_0)), \qquad T_0 = \frac{T_1 + T_2}{2}.$$

A static solution exists for equation (6):

$$\mathbf{u} = 0$$

$$T_s = T_0 - \frac{T_2 - T_1}{d} z$$

$$p_S = p_0 - \rho_0 \left(z + \gamma \frac{T_2 - T_1}{d} \frac{z^2}{2} \right) g$$

Using d as the length scale, $\frac{\kappa}{d^2}$ as time scale and $T_2 - T_1$ temperature scale, we introduce dimensionless variables

$$(x', y', z') = \frac{1}{d}(x, y, z), \qquad u'_i = \frac{d}{\kappa} u_i,$$

$$t' = \frac{\kappa}{d^2} t, \qquad T' = \frac{T}{T_2 - T_1}.$$

Assuming the mechanical dissipation $\Phi \approx 0$, and taking into account the temperature dependence of density only in the gravity term (Boussinesq approximation), we obtain from equations (6)

$$\nabla \cdot \mathbf{u} = 0\,, \tag{7a}$$

$$P^{-1}\left(\frac{\partial}{\partial t} + \mathbf{u}\cdot\nabla\right) = -\nabla\pi + R\Theta\hat{\mathbf{k}} + \nabla^2\mathbf{u}\,, \tag{7b}$$

$$(\partial t + \mathbf{u}\cdot\nabla)\,\Theta = \hat{\mathbf{k}}\cdot\mathbf{u} + \nabla^2\Theta\,, \tag{7c}$$

where primes have been dropped from the dimensionless variables and $\Theta = T' - T'_S$, $\pi = p' - p'_S$. Although there are seven dimensional parameters (ρ_0, g, γ, ΔT, ν, κ) that can be measured with four dimensions (namely m, s, kg, K), the mean density ρ_0 does not appear in the equations in the Boussinesq approximation so that only two dimensionless parameters are relevant for this problem. A first one is the Rayleigh number $R = \frac{\gamma g(T_2-T_1)d^3}{\nu\kappa}$. A second dimensionless number $P = \frac{\nu}{\kappa}$ is the Prandtl number. For small amplitude steady convection, we have

$$\nabla \cdot \mathbf{u} = 0\,, \tag{8a}$$

$$\nabla^2\mathbf{u} + R\theta\hat{\mathbf{k}} - \nabla\pi = 0\,, \tag{8b}$$

$$\nabla^2\Theta + \mathbf{u}\cdot\hat{\mathbf{k}} = 0\,. \tag{8c}$$

Operation with $-\hat{\mathbf{k}}\cdot\nabla\times\nabla\times$ on (8b) yields

$$\nabla^4 u_z + R\Delta_2\Theta = 0\,, \tag{9}$$

where

$$\Delta_2\, f = \left(\frac{\partial^2}{\partial x^2} + \frac{\partial^2}{\partial y^2}\right) f\,. \tag{10}$$

Take Δ_2 on equation 8c, and eliminate Θ from equation 9, we get a single equation of u_z:

$$\left(\nabla^6 - R\Delta_2\right) u_z = 0\,. \tag{11}$$

With the separation ansatz

$$\Delta_2 u_z = \left(\frac{\partial^2}{\partial x^2} + \frac{\partial^2}{\partial y^2}\right) u_z = -a^2 u_z\,, \tag{12}$$

equation (11) becomes

$$\left(\nabla^6 + R\,a^2\right) u_z = 0\,. \tag{13}$$

For stress-free boundaries, we have

$$u_z|_{z=\pm\frac{1}{2}} = 0,$$
$$\partial_z u_x|_{z=\pm\frac{1}{2}} = \partial_z u_y|_{z=\pm\frac{1}{2}} = 0,$$
$$\Theta|_{z=\pm\frac{1}{2}} = 0$$

Use the continuity equation $\partial_x u_x + \partial_y u_y + \partial_z u_z = 0$, we have

$$\partial_x \partial_z u_x + \partial_y \partial_z u_y + \partial_{zz}^2 u_z = \partial_{zz}^2 u_z = 0$$

at two boundaries. Also, from equation (9)

$$\left(\nabla^4 u_z + R\Delta_2 \Theta\right)|_{z=\pm\frac{1}{2}} = \partial_{zzzz}^4 u_z = 0$$

In summary, the stress-free boundary conditions are:

$$u_z = 0\,, \tag{14}$$
$$\partial_{zz}^2 u_z = 0\,, \tag{15}$$
$$\partial_{zzzz}^4 u_z = 0\,, \tag{16}$$

at $z = \pm\frac{1}{2}$. With these boundary conditions, equation (11) has solutions:

$$u_z = \cos ax \sin n\pi(z + \frac{1}{2})\,, \qquad n = 1, 2, 3, \dots\,, \tag{17}$$

and

$$R = \frac{(n^2\pi^2 + a^2)^3}{a^2}\,, \qquad n = 1, 2, 3, \dots\,. \tag{18}$$

a is the wavenumber of the unstable mode. The critical Rayleigh number R_c is the minimum of R, and is given when $n = 1$ and $a = \frac{\pi}{\sqrt{2}}$. Hence $R_c = \frac{27}{4}\pi^4$. Note that R_c is independent of the Prandtl number.

A single mode describes a roll of convection as sketched in figure 4. Because of the degeneracy of the unstable modes, complex behaviour can occur even close to the onset of instability and we will study it through a weakly non-linear analysis.

2 Weakly Non-linear Analysis

2.1 Perturbative Expansion

To illustrate the ideas of *weakly nonlinear analysis*, consider the following one dimensional example:

$$u''(z) + Ru(z) + u'(z)u(z) = 0 \quad \text{with} \quad u = 0 \text{ at } z = \pm\frac{1}{2}\,. \tag{19}$$

We make the ansatz

$$u = \epsilon u_1 + \epsilon^2 u_2 + \epsilon^3 u_3 + \,,$$
$$R = R_0 + \epsilon R_1 + \epsilon^2 R_2 + \dots\,,$$

and the normalization condition

$$\epsilon \equiv < u_1, u >= \epsilon < u_1, u_1 > + \epsilon^2 < u_1, u_2 > + \dots\,,$$

which is equivalent to

$$< u_1, u_n >= \delta_{1n} \qquad n = 1, 2, 3, \ldots .$$

Insert these ansatz into the original equations and collect terms according to the powers of ϵ. To the lowest order $O(\epsilon)$ we have

$$u_1'' + R_0 u_1 = 0\,,$$
$$u_1|_{z=\pm\frac{1}{2}} = 0\,.$$

The solutions are

$$u_1 = \sqrt{2}\sin n\pi\left(z + \frac{1}{2}\right), \quad \text{with } R_0 = n^2\pi^2, n = 1, 2, 3, \ldots$$

To continue the process, and for simplicity, we choose $n = 1$ here. Thus

$$u_1 = \sqrt{2}\sin\pi\left(z + \frac{1}{2}\right).$$

To the order $O(\epsilon^2)$,

$$u_2'' + R_0 u_2 = -u_1' u_1 - R_1 u_1$$

Multiply both sides with u_1 , integrate over the interval $-\frac{1}{2} \le z \le \frac{1}{2}$, we have on the left hand side:

$$< u_1(u_2'' + R_0 u_2) >=< u_2(u_1'' + R_0 u_1) >= 0$$

where integration by parts has been utilized. This condition yields

$$< -u_1(u_1' u_1 + R_1 u_1) >= 0 \Rightarrow R_1 = -\frac{< (u_1^3)' >}{3} = 0$$

which is the *solvability condition*. Now the equation of u_2 becomes

$$u_2'' + R_0 u_2 = -2\pi\sin\pi(z + \frac{1}{2})\cos\pi(z + \frac{1}{2}) \quad \text{with} \quad u_2|_{z=\pm\frac{1}{2}} = 0$$

The solution is

$$u_2 = \frac{\pi\sin 2\pi(z + \frac{1}{2})}{4\pi^2 - R_0} = \frac{\sin 2\pi(z + \frac{1}{2})}{3\pi}$$

To the third order of ϵ,

$$u_3'' + R_0 u_3 = -u_1' u_2 - u_2' u_1 - R_2 u_1 \quad \text{with} \quad u_3|_{z=\pm\frac{1}{2}} = 0$$

Apply the *solvability condition*, we have

$$\begin{aligned}
R_2 &= - < u_1(u_1' u_2 + u_2' u_1) > \\
&= - < \frac{1}{2} u_2 (u_1^2)' + u_2' (u_1^2) > \\
&=< \frac{1}{2} u_2 (u_1^2)' > \\
&= \frac{1}{4} \left\langle \frac{\pi^2 \sin 2\pi(z+\frac{1}{2}) \sin 2\pi(z+\frac{1}{2})}{3\pi^2} \right\rangle \\
&= \frac{1}{24}
\end{aligned}$$

In this simple example we are able to calculate the amplitude of the mode at saturation as a function of the departure from onset. At order ϵ^2 we get $\epsilon^2 R_2 = R - R_c$, so that

$$u \approx \epsilon\, u_1 = 4\sqrt{3}\,\sqrt{R - R_c}\, sin\, \pi \left(z + \frac{1}{2} \right) \tag{20}$$

In the case of convection close to onset of instability, the degeneracy of the unstable mode may lead to non trivial behaviour because many modes can interact. We will use a general formalism based on a weakly non-linear analysis similar to the simple one before. We write the Navier-Stokes equations and the temperature equations in the form

$$(\underline{\mathbf{W}} + R\,\underline{\mathbf{U}})\,\tilde{\mathbf{X}} = \frac{\partial}{\partial t}\underline{\mathbf{V}}\tilde{\mathbf{X}} + \mathbf{Q}(\tilde{\mathbf{X}}, \tilde{\mathbf{X}})\,, \tag{21}$$

where $\tilde{\mathbf{X}} = \begin{pmatrix} u_z \\ \theta \end{pmatrix}$ is a vector, $\underline{\mathbf{W}}$, $\underline{\mathbf{U}}$ and $\underline{\mathbf{V}}$ are linear operators, R is the control parameter and $\mathbf{Q}$ the non linear term.

We expand $\tilde{\mathbf{X}}$ and R in the form

$$\begin{aligned}
\tilde{\mathbf{X}} &= \epsilon\, \tilde{\mathbf{X}}_1 + \epsilon^2\, \tilde{\mathbf{X}}_2 + \ldots\,, \\
R &= R_0 + \epsilon\, R_1 + \epsilon^2\, R_2 + \ldots\,,
\end{aligned} \tag{22}$$

where ϵ is a small parameter and the other terms are of order one. We will now describe two aspects of the instability slightly above onset. We first focus on the steady pattern and then we study the dynamic interaction between the different modes that can lead to a kind of turbulence named phase turbulence.

2.2 Pattern selection

We write equation (21) at order ϵ and we recover the linear problem of steady convection. The solution is a linear combination of modes described by equation (17) with wave vectors of norm α. Thus, we write

$$\tilde{\mathbf{X}}_1 = \tilde{\mathbf{f}}(z) \sum_{n=-N}^{n=N} c_n\, e^{i\,\vec{k}_n.\vec{r}} \tag{23}$$

where $\vec{k}_n$ lies in the xy plane and is of modulus α. In order to have real solutions, we impose the two other relations $\vec{k}_{-n} = -\vec{k}_n$ and $c_{-n} = c_n^*$.

At order ϵ^2 we get

$$(\underline{\mathbf{W}} + R_0\,\underline{\mathbf{U}})\,\tilde{\mathbf{X}}_2 = \mathbf{Q}(\tilde{\mathbf{X}}_1, \tilde{\mathbf{X}}_1) - R_0\,\underline{\mathbf{U}}\,\tilde{\mathbf{X}}_1\,. \tag{24}$$

Then we apply the solvability condition $\langle \tilde{\mathbf{X}}_i^* | \text{right hand side} \rangle = 0$ where $\tilde{\mathbf{X}}_i^*$ is part of the kernel of the adjoint homogeneous linear operator. If the properties of the layer are symmetric with respect to the $z = 0$ plane, we obtain $R_1 = 0$ because $\mathbf{Q}$ is antisymmetric in z while $\tilde{\mathbf{f}}(z)$ and $\tilde{\mathbf{f}}^*(z)$ are symmetric. The solution of equation 24 can be written in the form

$$\tilde{\mathbf{X}}_2 = \sum_{i,k} \tilde{\mathbf{F}}(\vec{k}_i + \vec{k}_k,\, z)\, c_i\, c_k\, e^{i\,(\vec{k}_i+\vec{k}_k).\vec{r}}\,. \tag{25}$$

We write the equation (21) at order ϵ^3 and use the solvability condition. In the most general case, we get an expression of the form

$$\begin{aligned}\left(\epsilon\, R_1 + \epsilon^2\, R_2 + ...\right) U\, c_i^* = &- \beta\epsilon \sum_{n,m} c_n\, c_m\, \delta(\vec{k}_i + \vec{k}_n + \vec{k}_m) \\ &+ \epsilon^2 (\sum_{n=1}^{N} c_n\, c_n^*\, A(\vec{k}_i.\vec{k}_n) + A_0\, |c_i|^2)\, c_i^* \; + ... \text{ for i=1, 2, 3...}.\end{aligned} \tag{26}$$

Here β is an asymmetry coefficient which appears for instance if we consider non Boussinesq effects and write the temperature dependence of the density as
$\rho = \rho_0\,(1 - \alpha\,(T - T_0) + \beta\,(T - T_0)^2)$.
If $\beta = 0$, we get $R_1 = 0$ and we recover the symmetric case result.

Looking for regular solutions for which the angle between the N neighbouring q vectors is given by π/N and $|c_i|^2 = 1$, we obtain rolls solutions if $N = 1$, squares if $N = 2$. If $N = 3$ many solutions exists depending of the relative phases of the three coefficients c_i. In figure 4, these patterns of convection are sketched.

If $N \geq 4$ there are no regular periodic patterns but quasi patterns of higher order can be observed. Depending on the value of β and R, rolls or hexagons are stable. Without asymmetry or at high Rayleigh number, the rolls are stable whereas hexagons are stable if the asymmetry parameter β is high. Note that in some domain of the space parameters, both solution are stable, as can be seen in figure 5 [**?**, **?**, **?**].

2.3 Phase turbulence

We will now focus on the case where dynamic effects are present and try to describe how the different modes can interact. Using $C_i(t) = \epsilon c_i$, we write

$$\tilde{\mathbf{X}}(x, y, z, t) = \tilde{\mathbf{f}}(z) \sum_{n=-N}^{N} C_n(t)\, e^{i\,\vec{k}_n.\vec{r}} \tag{27}$$

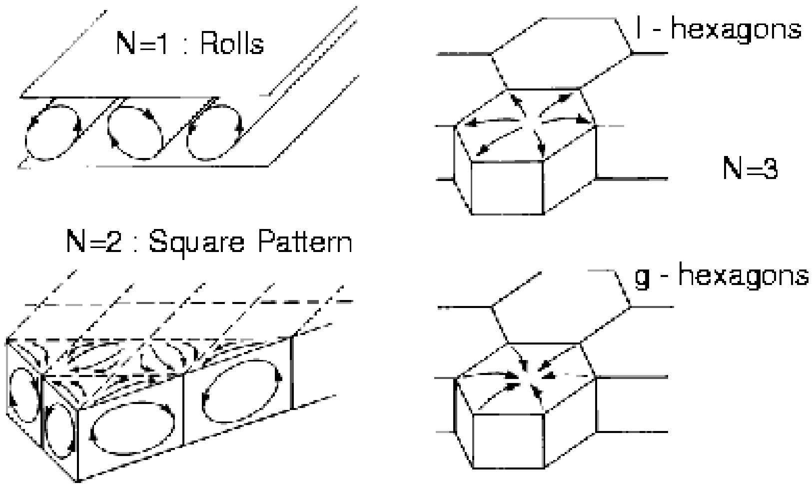

Figure 4: Sketch of patterns of convections: rolls, squares, l and g-hexagons.

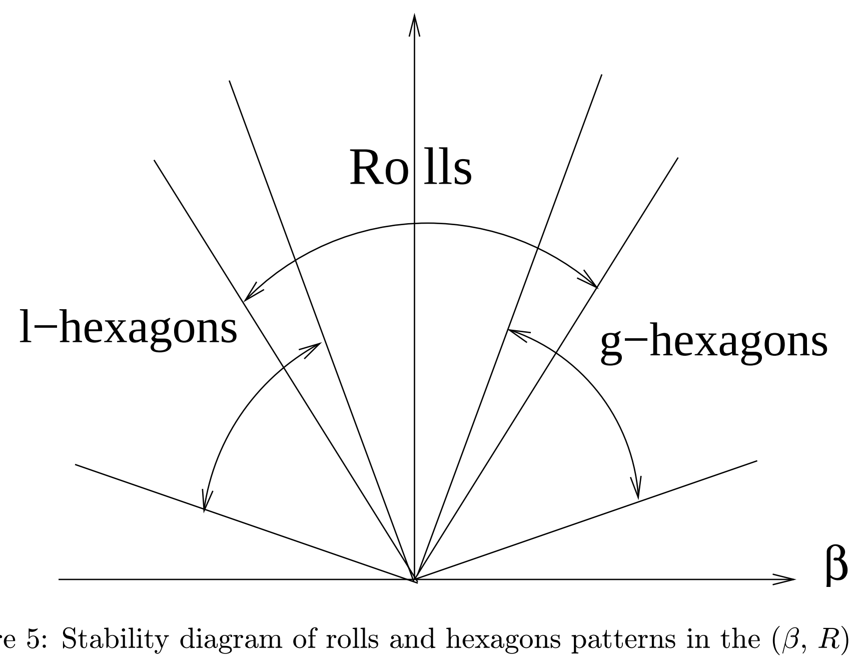

Figure 5: Stability diagram of rolls and hexagons patterns in the (β, R) plane.

Close to onset, one expects that the time dependence of the modes will be slow and of order ϵ^2. As before, we write the solvability condition at order three and this yields to dynamical equations for the coefficients

$$V\,\frac{d}{dt}C_i^* =(R-R_0)\,U\,C_i^* + \beta \sum_{n,m} C_n\,C_m\,\delta(\vec{k}_i + \vec{k}_n + \vec{k}_m) \tag{28}$$

$$+\,(\sum_{n=1}^{N} C_n\,C_n^*\,A(\vec{k}_i.\vec{k}_n) + E(\vec{k}_i.\vec{k}_n,\,\vec{\lambda}.\vec{k}_i\times\vec{k}_n) + A_0\,|C_i|^2)\,C_i^* \;+ \ldots \text{with i=1, 2, 3}\ldots. \tag{29}$$

If there is no rotation ($E = 0$), and if there is no mean flow, we can write the evolution equations at this order as

$$V\,\frac{d}{dt}C_i^* = -\frac{\partial}{\partial\,C_i}F(C_1, \ldots, C_n) \tag{30}$$

where

$$F(C_1, \ldots, C_n) = -\,\frac{1}{2}(R-R_0)\,U\sum_{i=1}^{N}|C_i|^2 - \frac{1}{3}\beta\sum_{i,n,m} C_i\,C_n\,C_m\,\delta(\vec{k}_i + \vec{k}_n + \vec{k}_m) \tag{31}$$

$$+\,\frac{1}{4}\left(\sum_{n=1}^{N}|C_n|^2\,A(\vec{k}_i.\vec{k}_n) +\,A_0\,|C_i|^2\right)|C_i|^2 \tag{32}$$

Thus these are evolution equations of Lyapunov type and the steady stable solutions will correspond to the local minima of F. The asymptotic approach is guaranteed and there can not be chaotic behaviour. This is not the case if either E is not equal to zero, or if we consider solutions with non-zero mean flow (stress free boundary) or if we consider terms of higher order. Then, chaotic behaviour can occur.

Indeed, when we consider a horizontal layer heated from below that is rotating about a vertical axis, E is not zero and the evolution equations are not of Lyapunov type. Above a critical value of the rotating parameter, all steady solutions become unstable. The local orientation of the convection rolls changes in time and this phenomenon is called phase turbulence. Experimental evidence have been seen in a rotating convection layer. A typical time evolution of the pattern of convection is shown in figure (6)[**?**, **?**].

Another case in which phase turbulence is present is the convection in the presence of stress-free boundaries. Because no stress is exerted by the boundaries on horizontal motion of the fluid, large scale flow can be generated by a small Reynolds stress. The advection of the pattern by the large scale mean flow must be taken into account in the evolution equations which are no longer of Lyapunov type. Phase turbulence can also occur as presented in figure 7 where the time evolution of the heat flux in convection is calculated numerically for different values of the Rayleigh number [**?**, **?**].

Phase turbulence shares some properties with the asymptotic turbulence of Navier-Stokes equations in the limit of infinite Reynolds number. A brief characterization of different types of turbulence is given in figure 8.

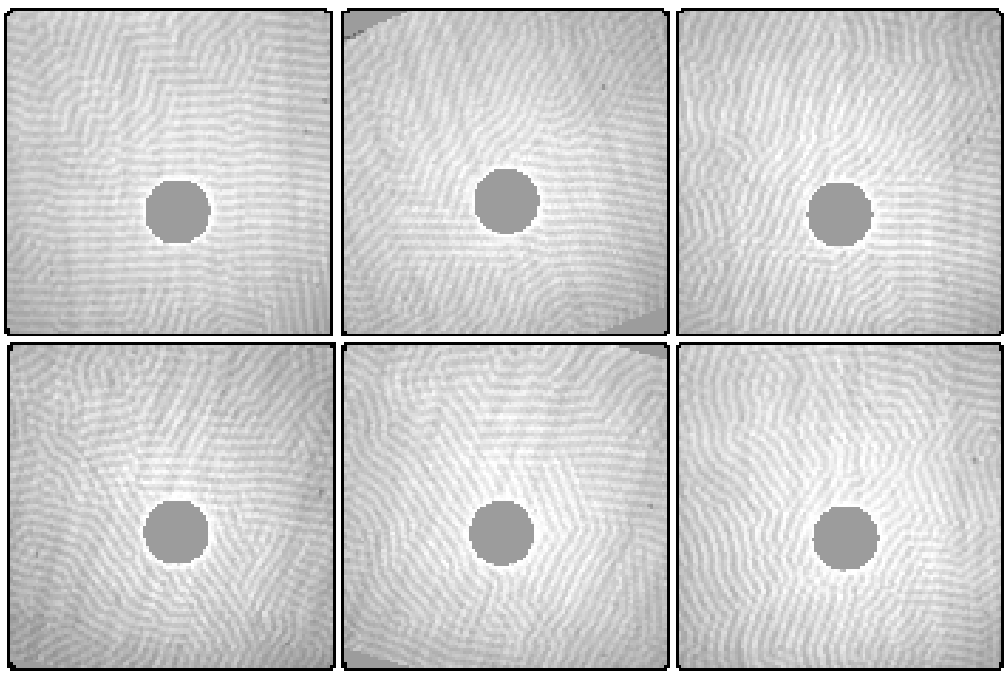

Figure 6: Time evolution of patterns of convection with phase turbulence [?, ?].

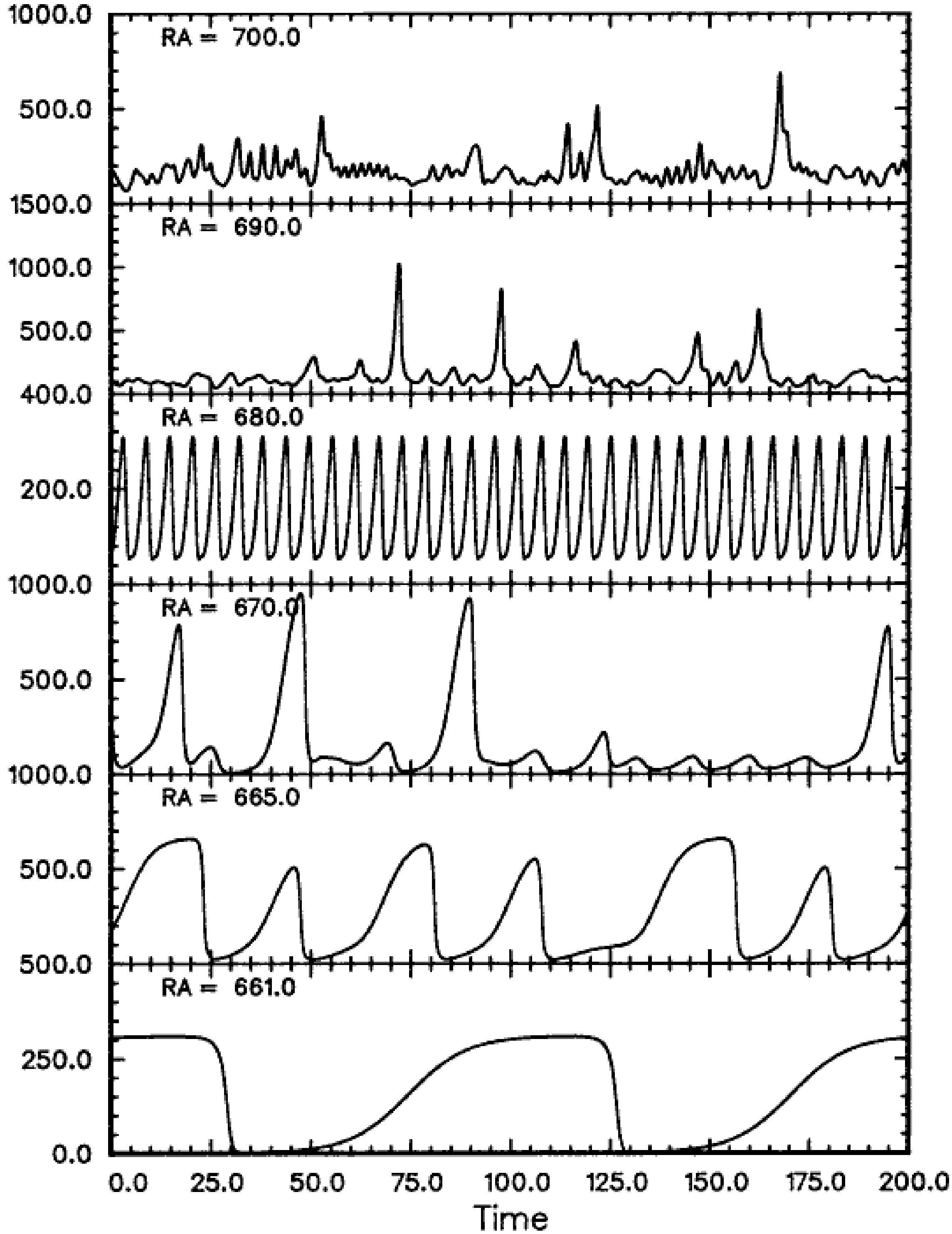

Figure 7: Time evolution of the heat flux for different values of the Rayleigh number and stress-free boundaries. $P_m = 0.15$. At high Rayleigh numbers the evolution is chaotic.

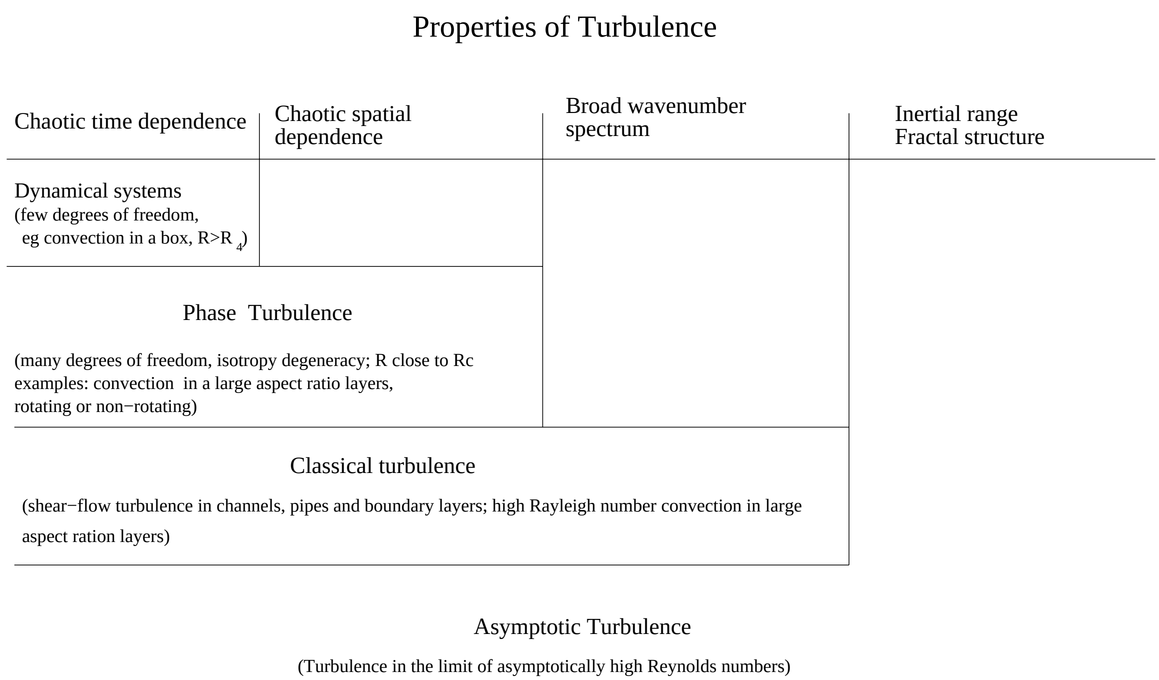

Figure 8: Characteristic properties of different kinds of turbulence.